

Observations of the Vela Pulsar Using VSOP

C.R. GWINN¹, J.E. REYNOLDS², D.L. JAUNCEY², A.K. TZIOUMIS²,
B. CARLSON³, S. DOUGHERTY³, D. DEL RIZZO³, H. HIRABAYASHI⁴,
H. KOBAYASHI⁴, Y. MURATA⁴, P.G. EDWARDS⁴, J.F.H. QUICK⁵,
C.S. FLANAGAN⁵ & P.M. MCCULLOCH⁶

¹ *UCSB, Santa Barbara, California 93106, USA*

² *ATNF, Epping, New South Wales, 2121, Australia*

³ *DRAO, Penticton, British Columbia, V2A 6K3, Canada*

⁴ *ISAS, Yoshinodai 3-1-1, Sagamihara, Kanagawa 229-8510, Japan*

⁵ *HRAO, Krugersdorp, Transvaal, South Africa*

⁶ *University of Tasmania, Hobart, 7001, Tasmania, Australia*

Abstract

Scattering in the interstellar plasma acts as an AU-scale lens to resolve the emission region of the Vela pulsar. In the observer plane, scattering produces a speckle pattern. Observations of this pattern on short baselines provide a measure of the size of the source. Observations on long baselines provide information about the spatial structure of the pulsar's emission region. Observations of this pattern for the Vela pulsar are in good agreement with theory, and should provide a picture of the Vela pulsar as a function of pulse phase.

1 Introduction

Pulsars exhibit rapid rotation and extremely strong gravitational and magnetic fields. This combination drives a strong electron-positron wind from near the surface of the star to beyond the light cylinder, where corotating material travels at lightspeed (Goldreich and Julian 1969). This wind may form the beam of radio waves that sweeps across the observer each rotation period, creating the observed pulses. Although this picture of pulsar magnetospheres is widely accepted, the physical mechanism, and even the location, of radio-wave generation remain unknown (Lyne and Graham-Smith 1998).

To improve understanding of pulsar emission mechanisms, we seek to resolve and image the pulsar's emission region. Scattering by plasma fluctuations in the interstellar plasma deflects radio waves, acting as

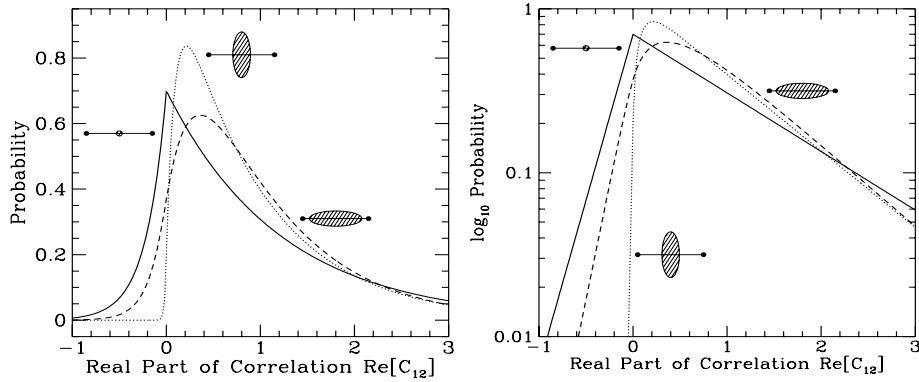


Figure 1: Expected distribution of the real part of the visibility, on a long baseline. Solid line: point source. Dotted line: source elongated perpendicular to baseline. Dashed line: elongated along baseline. Left panel: Linear scale. Right panel: Semilog scale.

an enormous, highly corrupt lens in interstellar space. In the plane of the observer, this lens produces a speckle pattern. Color Figure 9 shows an example of the speckle pattern for the Vela pulsar, observed on the HALCA-Tidbinbilla baseline. This pattern is the convolution of the point-source response with a diffraction-limited image of the source. The diffraction limit is set by the aperture of the scattering disk, the region in interstellar space from which the observer receives radiation (Gwinn et al. 1998). Because the angular size θ of the scattering disk increases with wavelength λ as $\theta \propto \lambda^2$, the linear resolution afforded by this technique actually increases with wavelength.

The Vela pulsar is an excellent candidate for speckle studies of pulsar structure, because it is strong, heavily scattered, and is an archetypical member of the class of young pulsars. It lies at a distance of about 500 pc. From ground-based observations, we have inferred a size for the pulsar of about 500 km (Gwinn et al. 1997, 2000). At 18 cm observing wavelength, the scattering disk has a diameter of about 3 AU (full width at half maximum of major axis). At the pulsar, the linear resolution of this “lens” is about 1000 km.

2 Statistics of the Speckle Pattern

In strong scattering, the observer receives radiation from a variety of paths, with relative phases differing by many turns. Consequently, the

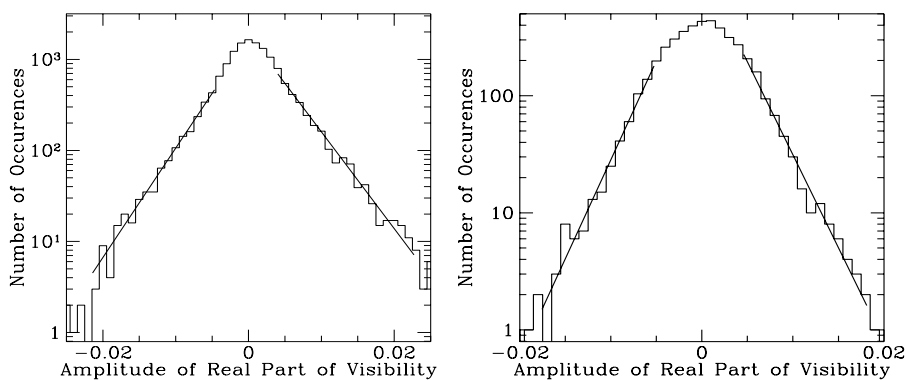


Figure 2: Distributions of amplitude of correlated flux density on a long baseline. Left: Hartebeesthoek-Tidbinbilla baseline. Right: HALCA-Tidbinbilla baseline. Each plot shows one fringe area, $4 \text{ MHz} \times 30 \text{ sec}$ for left plot and $4 \text{ MHz} \times 10 \text{ sec}$ for right.

electric field in the plane of the observer has statistics of a random walk. For a point source, the electric field is consequently drawn from a Gaussian distribution, and its square modulus, the intensity, is drawn from an exponential distribution (Goodman 1985). For a small but extended source, the distribution is a weighted sum of 3 exponentials; it resembles an exponential distribution with the small intensities missing (Gwinn et al. 1998).

On long baselines, correlated flux density of the source is the product of the electric fields at the 2 antennas. It is thus the product of factors drawn from 2 correlated Gaussian distributions. The distribution of the real part of the flux density can be shown to be a superposition of positive-going and a negative-going exponentials, along positive and negative directions. Figure 1 shows an example. If the source is resolved, the distribution becomes rounded near 0, and the scales of the exponentials change. The form of this change depends on the size of the source, the length of the baseline, and the orientation of the source relative to the baseline, if it is elongated.

3 Observations and Comparison with Theory

On 10 Dec 1997, we observed the Vela pulsar using HALCA and ground radio telescopes at Tidbinbilla (64-m diameter), Mopra (22-m), and Hartebeesthoek (26-m). We recorded data with the S2 recording sys-

tem. Tapes were analyzed at the LBA correlator in Australia to obtain a pulse ephemeris, and then correlated at the Canadian S2 correlator in Penticton. This analysis made heavy use of the capabilities of the Penticton correlator for high spectral resolution, rapid time sampling, pulsar gating, and extraordinarily careful treatment of statistics of input signals. The data were exported to UC Santa Barbara, where they were edited and fringed.

Figure 2 shows sample data for short time intervals, of one fringe area in each case. Because the scale is semilogarithmic, we expect the distributions to asymptotically approach straight lines, at amplitudes far from zero. As the figure shows, this is the case. Note also that the scales of the positive- and negative-going exponentials are different for the Hartebeesthoek-Tidbinbilla baseline, and are nearly the same for the longer HALCA-Tidbinbilla baseline. This is also in accord with predictions of the theory.

A solution for the structure of the pulsar will require fits to the distributions shown in Figure 2 including effects of noise and of averaging in frequency and time (Gwinn et al. 2000). This inversion will also benefit from measurements with the baseline at different position angles and with different lengths. The HALCA-Tidbinbilla baselines afford many such measurements, closely spaced in time, so that they are well suited to such an inversion. Efforts to image the pulsar using VSOP data, with resolution of hundreds of km, are underway.

Acknowledgements. We gratefully acknowledge the VSOP Project, which is led by the Japanese Institute of Space and Astronautical Science in cooperation with many organizations and radio telescopes around the world. We thank the US National Science Foundation for financial support.

References

- Goldreich, P., & Julian, W. H. 1969, *ApJ*, **157**, 869
Goodman, J.W. 1985, *Statistical Optics*, (New York: Wiley)
Gwinn, C.R., Britton, M.C., Reynolds, J.E. et al. 1998, *ApJ*, **505**, 928
Gwinn, C.R., Ojeda, M.J., Britton, M.C. et al. 1997, *ApJ*, **483**, L53
Gwinn, C.R., Britton, M.C., Reynolds, J.E. et al. 2000, *ApJ*, in press
Lyne, A.G., & Graham-Smith, F. 1998, *Pulsar astronomy*, 2nd ed. (Cambridge: Cambridge University Press)